Nuclear Engineering and Technology 49 (2017) 920–927

Contents lists available at ScienceDirect

Nuclear Engineering and Technology

journal homepage: www.elsevier.com/locate/net

Original Article

Dynamic Monte Carlo transient analysis for the Organization for Economic Co-operation and Development Nuclear Energy Agency (OECD/NEA) C5G7-TD benchmark

Nadeem Shaukat, Min Ryu, Hyung Jin Shim*

Seoul National University, 1 Gwanak-ro, Gwanak-gu, Seoul 08826, Republic of Korea

ARTICLE INFO

Article history:
Received 8 February 2017
Received in revised form
29 March 2017
Accepted 20 April 2017
Available online 26 May 2017

Keywords:
C5G7-TD
Dynamic Monte Carlo
McCARD
nTRACER
Transient Analysis

ABSTRACT

With ever-advancing computer technology, the Monte Carlo (MC) neutron transport calculation is expanding its application area to nuclear reactor transient analysis. Dynamic MC (DMC) neutron tracking for transient analysis requires efficient algorithms for delayed neutron generation, neutron population control, and initial condition modeling. In this paper, a new MC steady-state simulation method based on time-dependent MC neutron tracking is proposed for steady-state initial condition modeling; during this process, prompt neutron sources and delayed neutron precursors for the DMC transient simulation can easily be sampled. The DMC method, including the proposed time-dependent DMC steady-state simulation method, has been implemented in McCARD and applied for two-dimensional core kinetics problems in the time-dependent neutron transport benchmark C5G7-TD. The McCARD DMC calculation results show good agreement with results of a deterministic transport analysis code, nTRACER.

1. Introduction

The transient analysis of a nuclear reactor is one of the ultimate goals of Monte Carlo (MC) neutron transport calculations. Recently, MC transient analyses have been conducted using two kinds of approaches: the dynamic MC (DMC) method with the simulation of delayed neutron precursors [1,2] and the quasi-static method [3] in which MC neutron transport calculations are used to estimate the angular neutron flux at fixed time. The quasistatic method is used to efficiently solve a transient problem, but it may suffer from time-discretization approximation. The time-dependent MC (TDMC) methods, including the DMC method, can handle the time variable of the neutron density or flux in its continuous domain by updating event times during MC neutron tracking.

Since Kaplan [4] proposed an efficient matrix method utilizing TDMC neutron tracking to estimate the time constant or α-eigenvalue of a nuclear system in 1958, reactor analysis applications of TDMC methods have been limited to MC simulations of research reactors, including critical assemblies, to obtain kinetic physics parameters such as the α-eigenvalue, kinetics parameters, noise data, etc. KENO-NR, a variant of KENO-V.a [5], and MCNP [6] were used [7–9] to generate time-dependent detector responses in numerical simulations of noise experiments and pulsed neutron source experiments. The TART code [10] is equipped with a TDMC algorithm in which the time domain is split into time bins and the neutron population in each time bin is controlled using the combing technique [11,12]. Cullen et al. [12] compared the α-eigenvalues estimated by TART's TDMC calculations with those obtained using the α-static algorithm [13] for Godiva-like problems. For experimental benchmarks on a thorium-loaded accelerator-driven system [14], Shaukat and Shim [15] compared the α-eigenvalues calculated by the TDMC method and the α-iteration algorithm [16] using McCARD [17] with the experimental results. The Godiva super-prompt-critical burst experiment was simulated using the Serpent-OpenFoam coupled system considering thermal feedback [18].

As noted by Sjenitzer and Hoogenboom [1], the challenges of MC reactor transient analysis include effective generation of delayed neutrons, neutron population control, modeling of initial conditions, etc. As delayed neutrons play an important role in the transient behavior of reactor core characteristics, in spite of their small generation fraction from a fission reaction, a special treatment of their time-dependent generation is required to reduce the statistical uncertainty, which is expected to be high in direct sampling of their delayed-generation time at each fission site. In order to overcome

* Corresponding author.
E-mail address: shimhj@snu.ac.kr (H.J. Shim).

http://dx.doi.org/10.1016/j.net.2017.04.008

this problem, Sjenitzer and Hoogenboom [1] developed a clever algorithm of MC tracking and forced decay of delayed neutron precursors. The second issue of neutron population control has been approached in two ways in terms of simulations of the branching processes such as the fission reaction: an analog MC simulation in which extra neutrons from fission are sampled and tracked, accompanied by a time bin-wise population control technique such as the combing algorithm and the branchless method [1] in which the neutron weight is increased in accordance with the expected number of fission neutrons at each collision site. In this study, we apply Sjenitzer and Hoogenboom's delayed neutron handling algorithm and the analog MC branching process simulation method with the combing technique [12] for the DMC transient analysis.

For the modeling of the initial condition of a transient scenario, which is generally the steady-state condition, one may use the MC power iteration method [19] to obtain the fundamental-mode distribution of initial source neutrons and the fundamental-mode eigenvalue, k, as Sjenitzer and Hoogenboom [1] suggested. In this paper, as an alternative to the MC eigenvalue calculation, we propose a TDMC steady-state simulation method that is consistent with the DMC transient simulation method for the steady-state initial condition modeling. The DMC algorithms, including the proposed steady-state simulation method, have been implemented in McCARD [17] and applied for a time-dependent neutron transport benchmark based on the well-known steady-state C5G7 benchmark problems, in short the C5G7-TD benchmark [20]. The McCARD DMC results for the C5G7-TD benchmark are compared with those obtained using a deterministic transport analysis code, nTRACER [21].

2. TDMC steady-state simulation

As we apply existing methods for the delayed neutron generation [1] and neutron population control [12] in this DMC transient analysis, a new MC steady-state calculation method based on TDMC tracking is focused on in this section.

The main difference between the TDMC simulation and MC eigenvalue calculation [19] is that the former applies the exact collision kernel, C, at each collision site, while the latter applies the scattering collision kernel, C_s; these values are defined as follows:

$$C(\mathbf{r}';E',\mathbf{\Omega}'\rightarrow E,\mathbf{\Omega}) = \sum_r \nu_r(\mathbf{r}',E')\cdot\frac{\Sigma_r(\mathbf{r}',E')}{\Sigma_t(\mathbf{r}',E')}\cdot f_r(E',\mathbf{\Omega}'\rightarrow E,\mathbf{\Omega}) \tag{1}$$

$$C_s(\mathbf{r}';E',\mathbf{\Omega}'\rightarrow E,\mathbf{\Omega}) = \sum_{r\neq fis.} \nu_r(\mathbf{r}',E')\cdot\frac{\Sigma_r(\mathbf{r}',E')}{\Sigma_t(\mathbf{r}',E')}\cdot f_r(E',\mathbf{\Omega}'\rightarrow E,\mathbf{\Omega}) \tag{2}$$

ν_r is the average number of neutrons produced from a reaction of type r, and $f_r(E',\mathbf{\Omega}'\rightarrow E,\mathbf{\Omega})dEd\mathbf{\Omega}$ is the probability that a collision of type r by a neutron of direction $\mathbf{\Omega}'$ and energy E' will produce a neutron in direction interval $d\mathbf{\Omega}$ about $\mathbf{\Omega}$ with energy in dE about E. Other notations follow standard. By comparing Eqs. (1) and (2), one can see that the only difference is whether the fission reaction is sampled or not. The fission reaction can be sampled in the reaction-type sampling process of the TDMC method, as is the case in the MC fixed-source-mode calculations, while the fission reaction is discarded in the MC power iteration method. Then, the ignored fission reaction in the reaction-type sampling process is considered by sampling fission source neutrons for the next iteration (or cycle) MC simulations with probability of $w\cdot\left(\frac{\nu_f(\mathbf{r}',E')}{k}\right)\cdot\left(\frac{\Sigma_f(\mathbf{r}',E')}{\Sigma_t(\mathbf{r}',E')}\right)$, where w

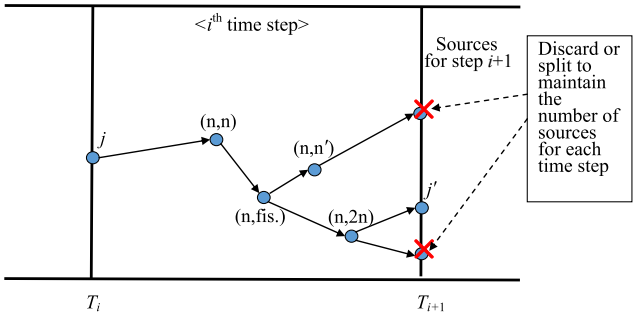

Fig. 1. Example of an MC history simulation at time step i. MC, Monte Carlo.

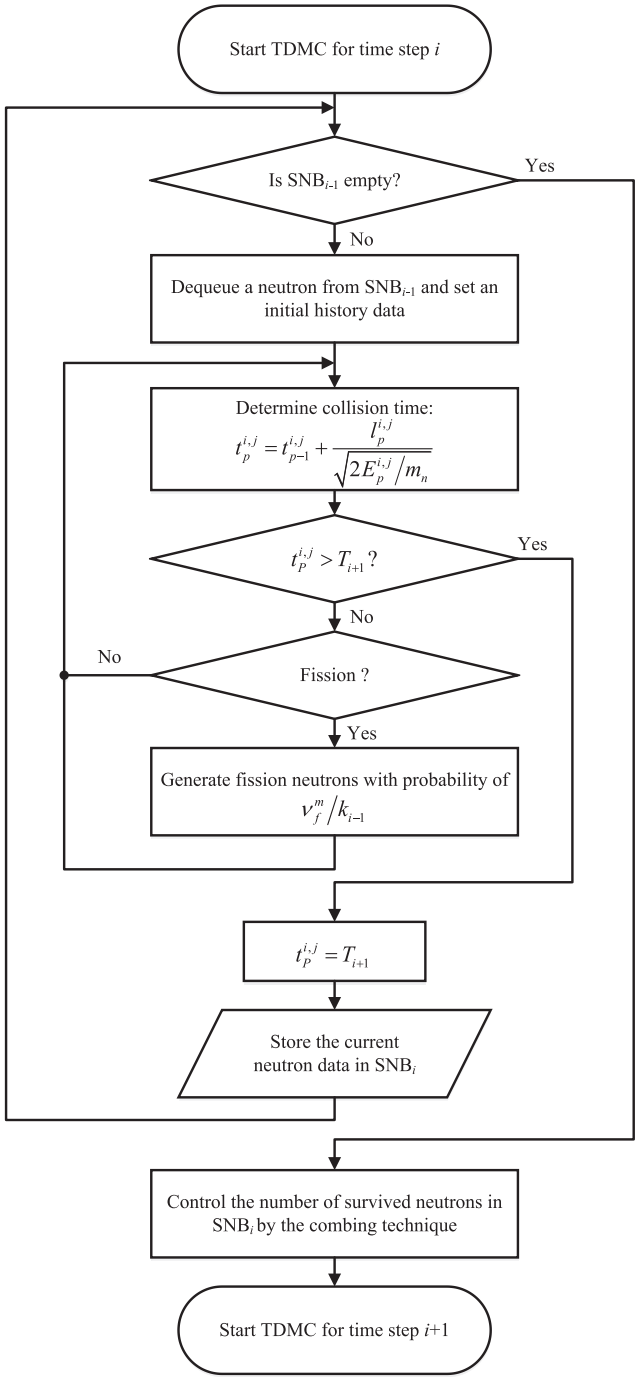

Fig. 2. Flow chart of the TDMC steady-state calculation at time step i. SNB_i, surviving neutron bank stored at the end of time step i; TDMC, time-dependent Monte Carlo.

and ν_f are the neutron weight and the average number of total fission neutrons per fission reaction at the collision site, respectively. In this MC power iteration algorithm, the division by k in the fission neutron production probability plays the role of source normalization iteration by iteration (or cycle by cycle). As is well known [22,23], this replacement of ν_f by a fictitious value, ν_{fic}, defined by ν_f/k, is the only alteration of the eigenvalue equation for the steady-state analysis from the physical system.

By making the best of this concept of $\nu_{fic.}$, steady-state distributions of fission sources and delayed neutron precursors, as well as k, can be obtained via TDMC simulations with slight modification. We suppose that the total number of time steps, the time step interval, the number of neutron histories, and an initial k value are provided in a user input for the TDMC steady-state calculations. In TDMC simulations with the combing technique [12], each neutron is simulated time step by time step with updating of its time variable whenever its track is sampled by the following equation:

$$t_p^{i,j} = t_{p-1}^{i,j} + \frac{l_p^{i,j}}{\sqrt{2E_p^{i,j}/m_n}}, \tag{3}$$

where $t_{p'}^{i,j}(p' = p \text{ or } p-1)$, $l_p^{i,j}$, and $E_p^{i,j}$ are, respectively, the time after the p'^{th} flight, the length, and the neutron energy of the p^{th} track, of history j at time step i; m_n is the neutron mass. If the sampled time is greater than the upper time bound of the i^{th} time step, i.e., $t_p^{i,j} > T_{i+1}$, then the track length of, and time after the last flight P, of history j, denoted by $l_P^{i,j}$ and $t_P^{i,j}$, respectively, become the following:

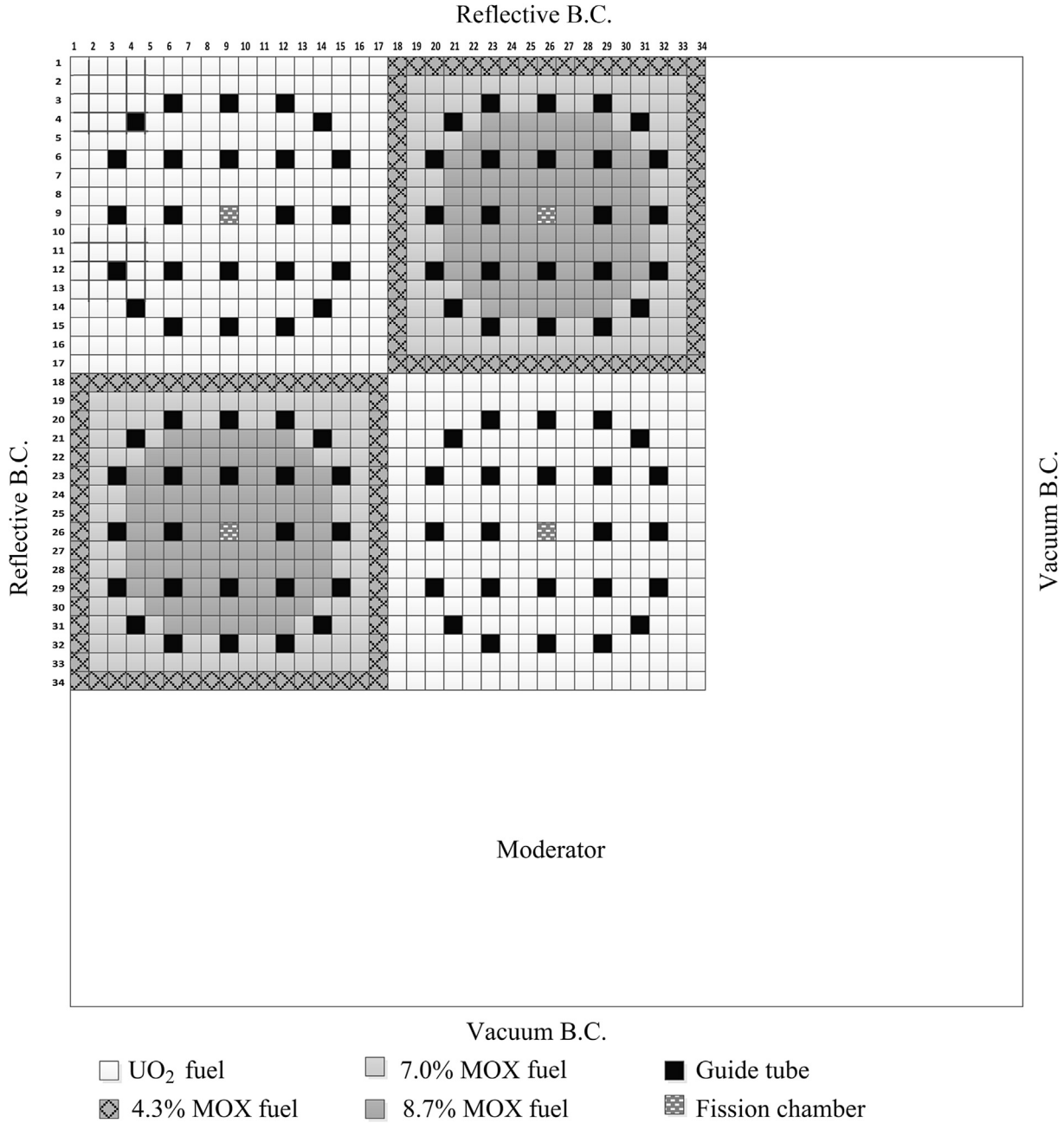

Fig. 3. 2D core configuration for the C5G7-TD benchmark. BC, boundary condition; MOX, mixed oxide; UO_2, uranium dioxide; 2D, two dimensional.

$$l_P^{i,j} = \left(T_{i+1} - t_{P-1}^{i,j}\right) \cdot \sqrt{2E_P^{i,j}/m_n}, \quad (4)$$

$$t_P^{i,j} = T_{i+1}, \quad (5)$$

where $E_P^{i,j}$ indicates the neutron energy of the last flight of history j at time step i. After the i^{th} time step TDMC simulations for all histories, the number of neutrons for the next time step simulations are controlled to be the user-provided number of histories obtained by the Russian roulette or splitting method depending on the number of surviving neutrons at T_{i+1}. Fig. 1 shows an example of a simulated neutron history at time step i.

In this TDMC simulation with population control, the only modification necessary to obtain the fundamental-mode distributions of fission sources and delayed neutron precursors is to generate as many fission neutrons as ν_f^m/k_{i-1}, where ν_f^m and k_{i-1} are the average number of total fission neutrons per fission of isotope m and the eigenvalue estimated at the time step $(i-1)$, when a fission reaction of isotope m is selected during the MC simulations. From each time step TDMC simulation, k can be estimated by calculating the ratio between the amounts of fission neutron production and net losses of neutrons.

Then, after the modified TDMC simulations for the user-provided number of time steps, which is supposed to be sufficient to converge the fission source distribution, initial fission sources for the DMC transient simulation are determined as surviving neutrons at the end of these TDMC steady-state calculations. Initial sites of the delayed neutron precursors are selected with the probability of $w \cdot \nu_d(\mathbf{r}', E') \cdot \left(\frac{\Sigma_f(\mathbf{r}', E')}{\Sigma_t(\mathbf{r}', E')}\right)$, where ν_d is the number of delayed neutrons per fission reaction at every collision site during the last time step TDMC simulations while applying the population control technique of the delayed neutron precursors [1].

Fig. 2 shows an algorithm of the TDMC steady-state calculations at the i^{th} time step. In the figure, $SNB_{i'}$ ($i' = i$ or $i-1$) indicates a data structure for storing surviving neutrons at time $T_{i'+1}$.

3. C5G7-TD application results

For the verification of transient analysis codes, the C5G7-TD benchmark [20] specifies a series of space–time neutron kinetics problems without consideration of any feedback effects. The C5G7-TD benchmark problems are based on the well-studied steady-state C5G7 specification [24] and additionally define physical constants related to delayed neutron characteristics. The benchmark's two-dimensional (2D) core configuration is the same as that of the C5G7 core, consisting of 16 fuel assemblies (FAs)—eight UO_2 FAs and eight mixed oxide FAs, as shown in Fig. 3. Each 17 × 17 FA has 264 fuel pins, 24 guide tubes (GTs) for control rods (CRs), and one instrument tube (IT) for the fission chamber (FC) in the center grid cell. Every pin cell with pitch of 1.26 cm is modeled by two regions—a cylinder with radius 0.54 cm for a mixture region of fuel-clad, moderator-filled GT, CR-GT, or FC-IT, and a surrounding moderator region. There are four CR banks, each of which governs CRs in FAs at the same position in the quarter symmetry. Bank numbers of 1, 2, 3, and 4 are assigned to the north-west, north-east, south-west, and south-east FAs, respectively, as shown in Fig. 3.

The C5G7-TD benchmark provides four exercise sets from 0 to 3 in the 2D configuration, and two exercise sets of 4 and 5 in 3D geometry. Transient events in the 2D problem sets can be modeled by time-dependent changes of the seven-group macroscopic cross sections in the CR-GT mixture regions. In this paper, McCARD DMC calculation results for the four 2D problem sets are presented and verified via comparisons with those calculated by the deterministic code nTRACER [21]. The McCARD DMC calculations for the 2D benchmark problems are performed from 0 s to 3 s with time intervals of 0.05 milliseconds using 100,000 neutron histories.

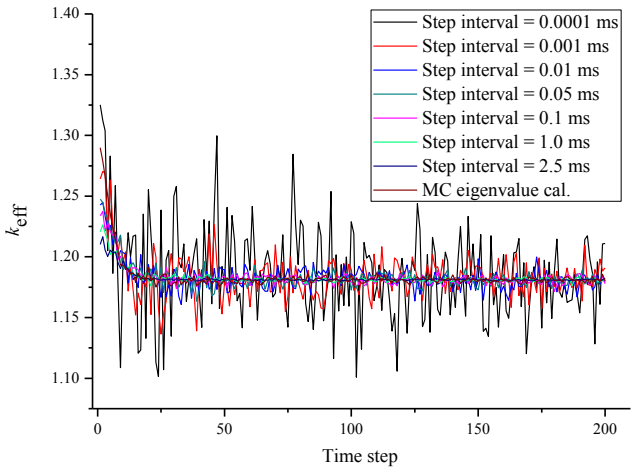

Fig. 4. The k_{eff} convergence plots of the TDMC steady-state calculations for 2D C5G7-TD, varying the time step interval from 0.0001 milliseconds to 10 milliseconds. cal. = calculations; TDMC, time-dependent Monte Carlo; 2D, two dimensional.

3.1. TDMC steady-state calculation

The TDMC steady-state simulation is newly proposed to generate initial prompt neutron sources and delayed neutron precursors for the DMC transient simulations. In order to investigate the effect of the time step interval, TDMC steady-state calculations during 200 time steps are performed with varying of the interval, such as 0.0001 milliseconds, 0.001 milliseconds, 0.01 milliseconds, 0.05 milliseconds, 0.1 milliseconds, 1.0 milliseconds, and 2.5 milliseconds, considering that the prompt neutron generation time is estimated by the MC adjoint-weighted kinetics parameter estimation method [17] to be about 0.014 milliseconds. Fig. 4 shows convergence plots of the fundamental-mode eigenvalue k_{eff} by the TDMC steady-state simulations with changing of the step interval. From the figure, it can be seen that k_{eff} converges after 50 time steps with step intervals larger than 0.01 milliseconds, while k_{eff} values with

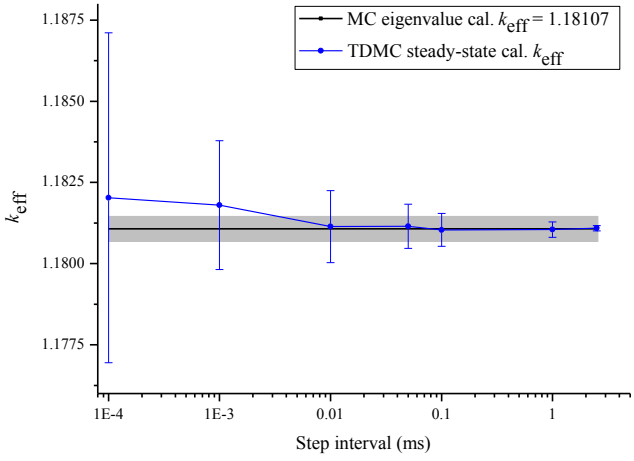

Fig. 5. Comparison of converged k_{eff} values calculated by the TDMC steady-state simulations for 2D C5G7-TD according to the time step interval. cal. = calculations; TDMC, time-dependent Monte Carlo; 2D, two dimensional.

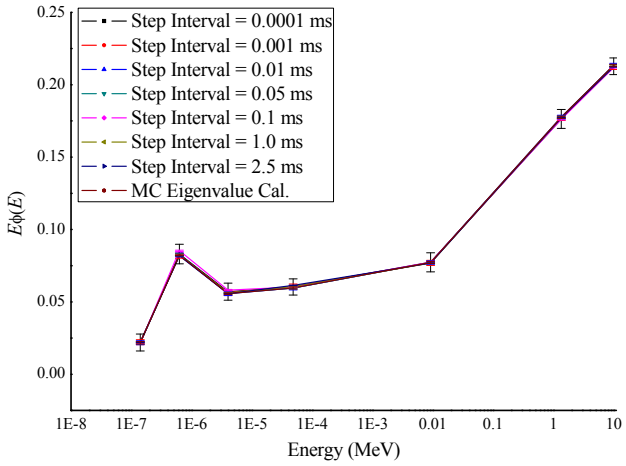

Fig. 6. Comparison of flux spectra with varying the time step interval in the TDMC steady-state simulations for the 2D C5G7-TD core. cal. = calculations; TDMC, time-dependent Monte Carlo; 2D, two dimensional.

small step intervals of 0.0001 milliseconds and 0.001 milliseconds fluctuate more than those with bigger intervals. Fig. 5 shows a comparison of the converged k_{eff}' values calculated by averaging the estimated k_{eff} values from the 51st to the 200th time step with a reference from the standard MC eigenvalue calculation method [19]. The error bars in Fig. 5 indicate the ±2 standard deviation (SD) intervals of the mean values, where the SDs are calculated by the square root of the sample variance from the time step-wise k_{eff} values of the TDMC steady-state calculations and the gray area from the cycle-wise k_{eff} estimates in the MC eigenvalue calculation. From the figure, one can see that the proposed TDMC steady-state calculation, with a sufficiently large time step interval, can predict k_{eff} within its confidence intervals, which become larger as the time step interval becomes smaller. Fig. 6 shows comparisons of the flux spectra in the TDMC steady-state calculations with that from the MC eigenvalue calculation. In the figure, the flux spectra coincide with each other very well. From these results, the time step interval of the TDMC steady-state calculations in this study is selected to be 0.05 milliseconds, which is about 3.5 times larger than the prompt neutron generation time.

3.2. C5G7 Exercise 0

In problem set C5G7 Exercise 0 (TD0), a postulated instantaneous CR insertion and withdrawal transient of designated CR banks is modeled by step changes of the cross sections of the GT mixture regions, Σ^{GTM}, during 2 s as follows:

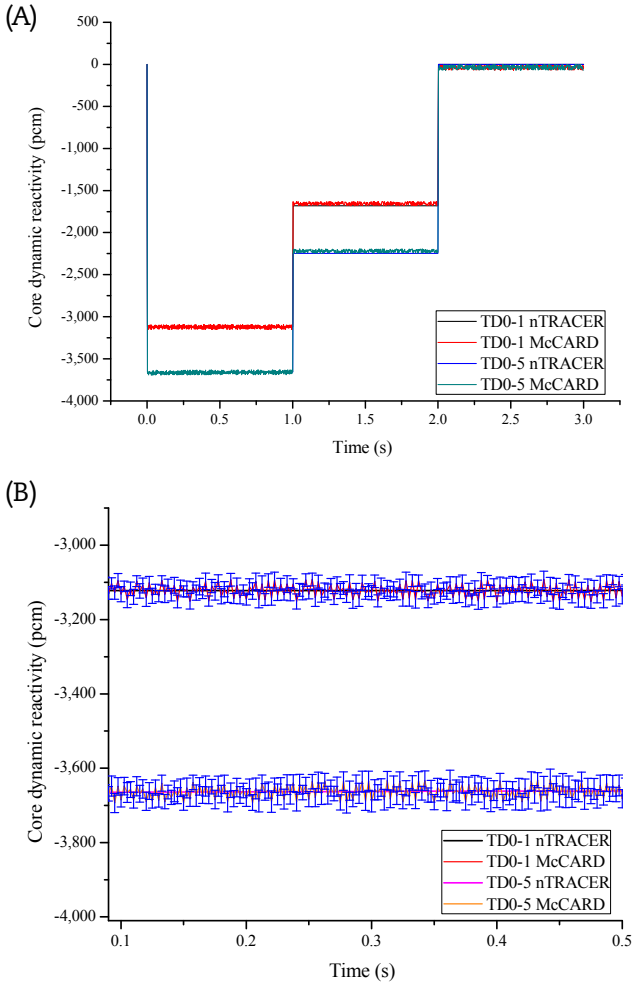

Fig. 7. Comparisons of dynamic reactivities calculated by McCARD and nTRACER for problems TD0-1 and TD0-5. (A) 0 s ≤ t ≤ 3 s (B) 0.1 s ≤ t ≤ 0.5 s.

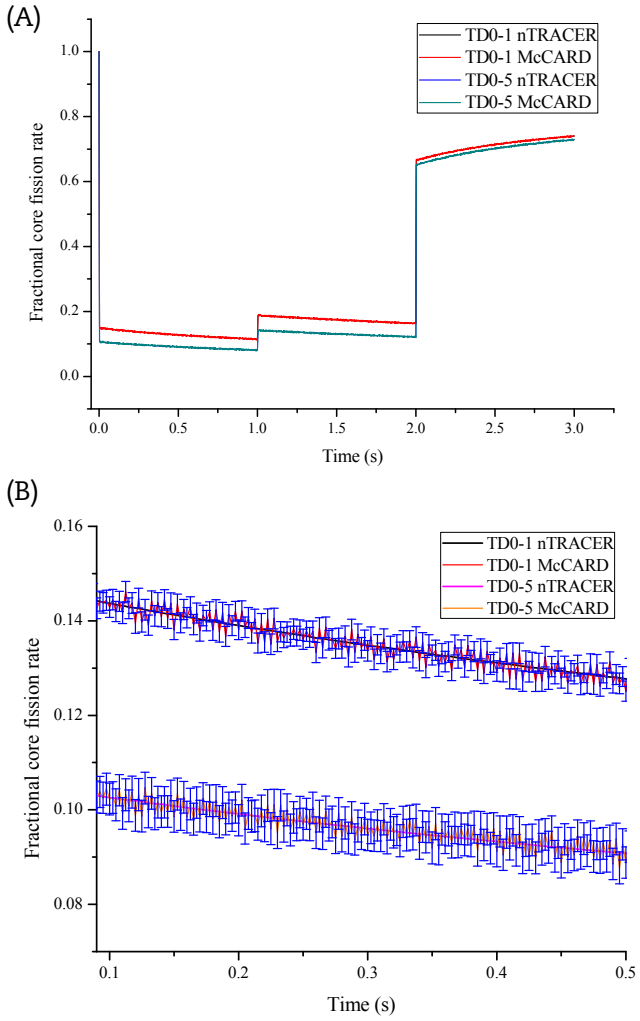

Fig. 8. Comparisons of fractional total fission rates calculated by McCARD and nTRACER for problems TD0-1 and TD0-5. (A) 0 s ≤ t ≤ 3 s (B) 0.1 s ≤ t ≤ 0.5 s.

$$\Sigma_{rg}^{GTM}(t) = \begin{cases} \Sigma_{rg}^{GT}; & t = 0,\ t \geq 2\ \text{s} \\ \Sigma_{rg}^{GT} + 0.1\left(\Sigma_{rg}^{R} - \Sigma_{rg}^{GT}\right); & 0\ \text{s} < t \leq 1\ \text{s} \\ \Sigma_{rg}^{GT} + 0.05\left(\Sigma_{rg}^{R} - \Sigma_{rg}^{GT}\right); & 1\ \text{s} \leq t < 2\ \text{s} \end{cases} \quad (6)$$

where r and g are the reaction type and energy group indices, respectively. The superscripts GT and R represent the moderator-filled GT and the CR-GT composition, respectively.

Among the five problems in TD0, the McCARD DMC calculations are performed for TD0-1 and TD0-5, where the postulated CR movements of Bank 1 and all the banks, respectively, occur. Fig. 7 shows comparisons of the core dynamic reactivities calculated by McCARD and nTRACER for problems TD0-1 and TD0-5. From Fig. 7A, one can observe abrupt decreases of reactivity at 0 s due to sudden insertion of CRs, constant reactivities until 1 s, sudden increases at 1 s due to moving of the CRs to the half position of inserted length, and restorations at 2 s due to withdrawing of the CRs to the initial positions. Fig. 7B magnifies the comparisons in a range between 0.1 s and 0.5 s with ±2 SD intervals of the mean estimates over the tally interval of 2.5 milliseconds, where the SD is calculated by the sample SD from the history-wise estimates during each 2.5 milliseconds. Fig. 8 shows comparisons of the fractional total core fission rates, defined by the fraction of the total core

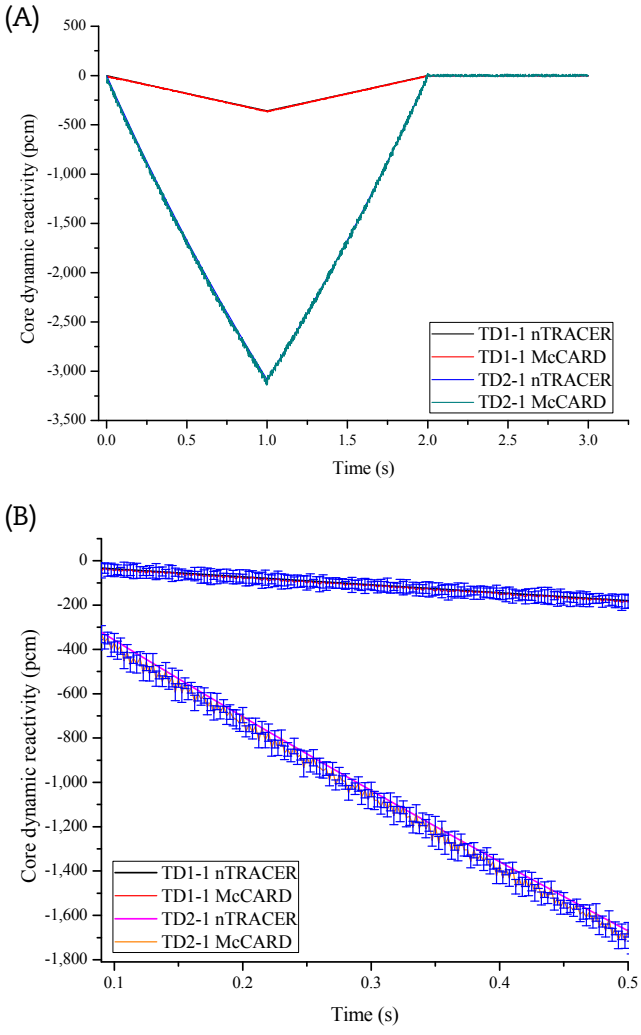

Fig. 9. Comparisons of dynamic reactivities calculated by McCARD and nTRACER for problems TD1-1 and TD2-1. (A) 0 s ≤ t ≤ 3 s (B) 0.1 s ≤ t ≤ 0.5 s.

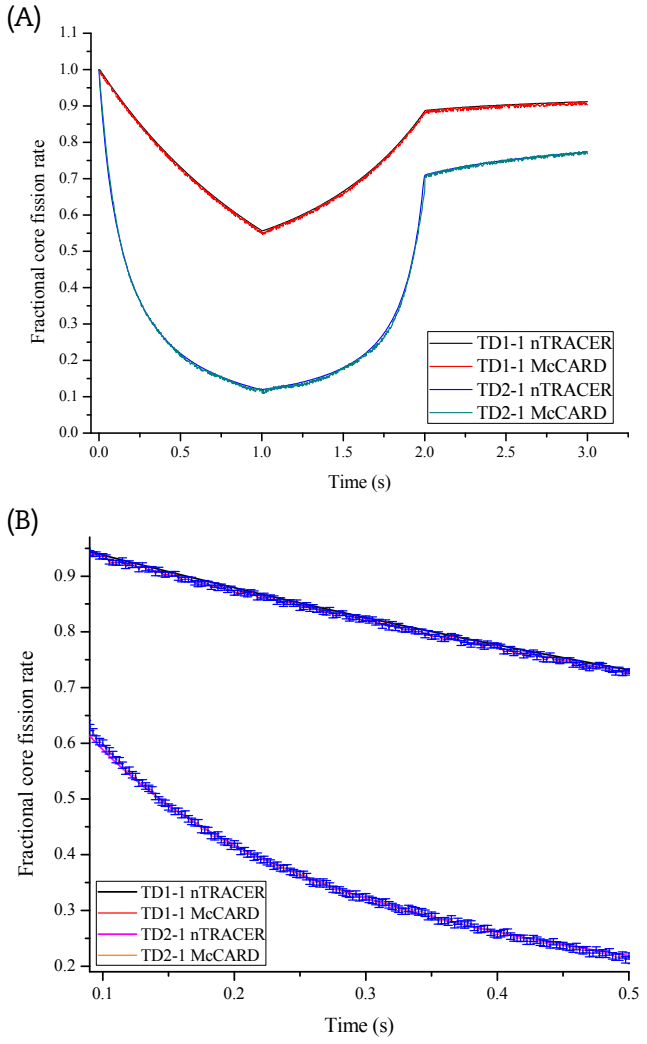

Fig. 10. Comparisons of fractional total fission rates calculated by McCARD and nTRACER for problems TD1-1 and TD2-1. (A) 0 s ≤ t ≤ 3 s (B) 0.1 s ≤ t ≤ 0.5 s.

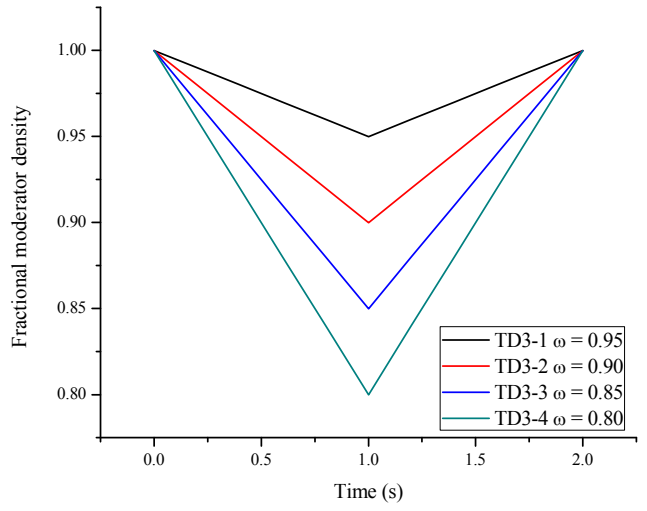

Fig. 11. Core moderator density changes in TD3 problems.

fission rate to its initial value at 0 s, calculated by McCARD and nTRACER for problems TD0-1 and TD0-5. From the figures, one can see that the McCARD DMC calculation results agree well with those of nTRACER.

3.3. C5G7 Exercises 1 and 2

Exercises 1 and 2 (TD1 and TD2, respectively) represent core transients due to CR insertion and extraction at a constant speed. In both problem sets, the cross sections of the GT region are defined by the following equation:

$$\Sigma_{rg}^{GTM}(t) = \begin{cases} \Sigma_{rg}^{GT} + \alpha\left(\Sigma_{rg}^{R} - \Sigma_{rg}^{GT}\right)t; & 0\ \text{s} \le t < 1\ \text{s} \\ \Sigma_{rg}^{GT} + \alpha\left(\Sigma_{rg}^{R} - \Sigma_{rg}^{GT}\right)(2-t); & 1\ \text{s} \le t < 2\ \text{s} \\ \Sigma_{rg}^{GT}; & t \ge 2\ \text{s} \end{cases} \quad (7)$$

where α is the cross-section change rate, whose value is 0.01 for TD1 and 0.1 for TD2. Figs. 9 and 10 show comparisons of dynamic reactivities and fractional total fission rates, respectively, calculated by McCARD and nTRACER for TD1-1 and TD2-1 while considering the CR movements in Bank 1. From Fig. 9, one can observe that reactivity linearly decreases from 0 s to 1 s and increases after 1 s until 2 s due to ramp changes of the cross sections at the GT regions, as shown in Eq. (7). From the figures, one can see that the McCARD DMC calculation results agree well with those of nTRACER for cases TD0-1 and TD0-5.

3.4. C5G7 Exercise 3

Exercise 3 (TD3) is designed for the transient event of a change in the core moderator density. Fig. 11 illustrates four scenarios of time-dependent fraction changes of the moderator density. According to the density change profile, the time-dependent cross sections of the moderator Σ^{M3} in each TD3 problem can be expressed as follows:

$$\Sigma_{rg}^{M3}(t) = \begin{cases} \Sigma_{rg}^{M} - (1-\omega)\Sigma_{rg}^{M}t; & 0\ \text{s} \le t < 1\ \text{s} \\ (2\omega - 1)\Sigma_{rg}^{M} + (1-\omega)\Sigma_{rg}^{M}t; & 1\ \text{s} \le t < 2\ \text{s} \\ \Sigma_{rg}^{M}; & t \ge 2\ \text{s} \end{cases} \quad (8)$$

where ω is the minimum change fraction, for which the values are 0.95, 0.90, 0.85, and 0.80 for TD3-1, TD3-2, TD3-3, and TD3-4 cases, respectively. The superscript M indicates the moderator.

Figs. 12 and 13 show comparisons of dynamic reactivities and fractional total fission rates, respectively, calculated by McCARD

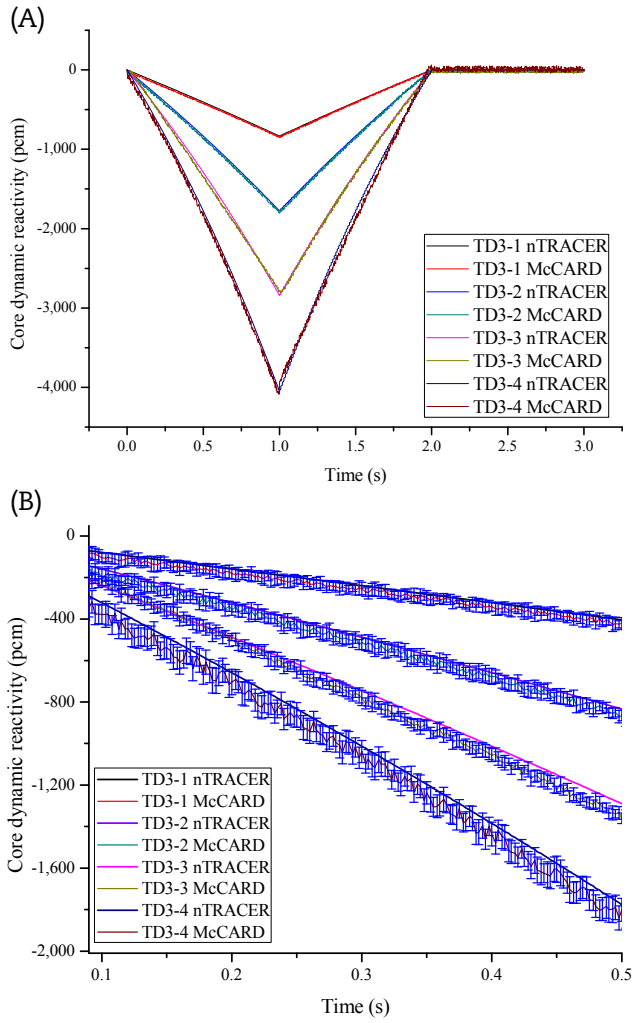

Fig. 12. Comparisons of dynamic reactivities calculated by McCARD and nTRACER for TD3 problems. (A) 0 s ≤ t ≤ 3 s (B) 0.1 s ≤ t ≤ 0.5 s.

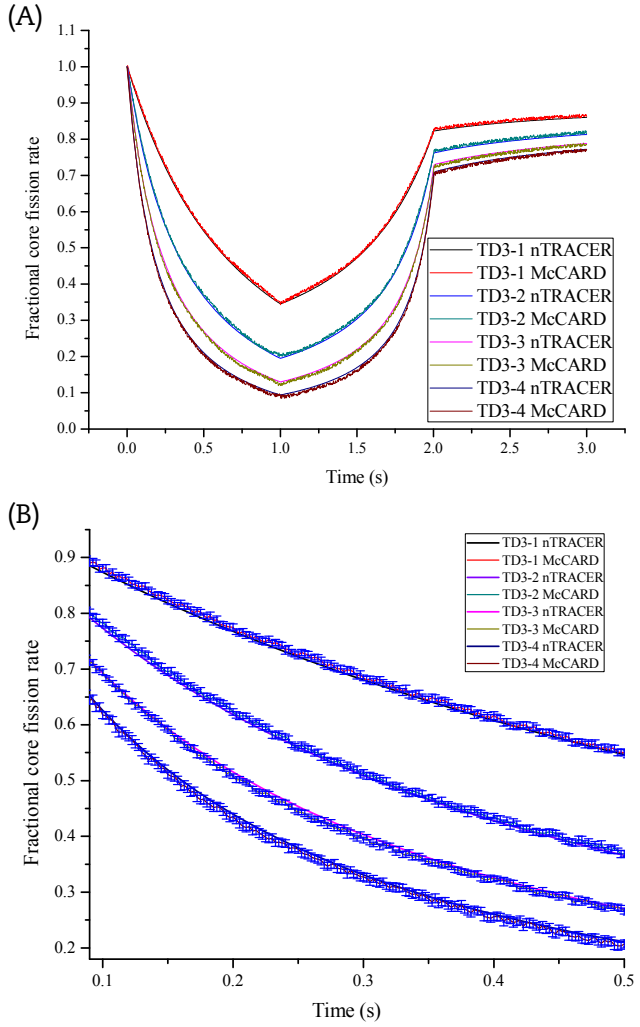

Fig. 13. Comparisons of fractional total fission rates calculated by McCARD and nTRACER for TD3 problems. (A) 0 s ≤ t ≤ 3 s (B) 0.1 s ≤ t ≤ 0.5 s.

and nTRACER for TD3 problems with changing ω. Fig. 12 illustrates that there are linear decreases of reactivities during the first 1 s and linear increases for the next 1 s because of linear changes of the moderator density, as shown in Fig. 11. From the figures, it is demonstrated that the McCARD DMC calculation results agree well with those of nTRACER.

4. Conclusions

We developed a new MC steady-state simulation suited to generate prompt neutron sources and delayed neutron precursors for DMC transient simulations. The proposed TDMC steady-state simulation method, accompanied by Sjenitzer and Hoogenboom's delayed neutron handling algorithm and the analog MC branching process simulation method with the combing technique, is applied for DMC analysis of 2D C5G7-TD kinetics problems. In the numerical results, it is demonstrated that the McCARD DMC results show excellent agreement with those obtained using the deterministic transport analysis code nTRACER.

Conflicts of interest

No conflicts of interest.

Acknowledgments

This research was supported by the National Nuclear R&D Program through the National Research Foundation of Korea funded by Ministry of Science, ICT and Future Planning (NRF-2014M2A8A1032047).

References

[1] B.L. Sjenitzer, J.E. Hoogenboom, Dynamic Monte Carlo method for nuclear reactor kinetics calculations, Nucl. Sci. Eng. 175 (2013) 94–107.
[2] B.L. Sjenitzer, J.E. Hoogenboom, J.J. Escalante, V.S. Espinoza, Coupling of dynamic Monte Carlo with thermal–hydraulic feedback, Ann. Nucl. Energy 76 (2015) 27–39.
[3] Y.G. Jo, B. Cho, N.Z. Cho, Nuclear reactor transient analysis by continuous-energy Monte Carlo calculation based on predictor-corrector quasi-static method, Nucl. Sci. Eng. 183 (2016) 229–246.
[4] E.L. Kaplan, Monte Carlo Methods for Equilibrium Solutions in Neutron Multiplication, UCRL-5275-T, Lawrence Livermore National Laboratory, 1958.
[5] L.M. Petrie, N.F. Cross, KENO-V.a: an Improved Monte Carlo Criticality Program with Supergrouping, NUREG/CR-0200, Sec. Fll, ORNL/NUREG/CSD-2 vol. 2, Oak Ridge National Laboratory, 1985.
[6] J.F. Briesmeister (Ed.), MCNP—A General Monte Carlo N-Particle Transport Code, Version 4A, LA-12625, Los Alamos National Laboratory, 1993.
[7] J.T. Mihalczo, T.E. Valentine, Calculational verification and process control applications utilizing the high sensitivity of noise measurement parameters to fissile system configuration, Nucl. Sci. Eng. 121 (1995) 286–300.
[8] T.E. Valentine, J.T. Mihalczo, MCNP-DSP: a neutron and gamma ray Monte Carlo calculation of source-driven noise-measured parameters, Ann. Nucl. Energy 23 (1996) 1271–1287.
[9] U. Wiącek, E. Krynicka, Decay of the pulsed thermal neutron flux in two-zone hydrogenous systems—Monte Carlo simulations using MCNP standard data libraries, Nucl. Instrum. Methods Phys. Res. B 243 (2006) 92–98.
[10] D.E. Cullen, TART 2002: a Coupled Neutron–photon, 3-D, Combinatorial Geometry, Time Dependent Monte Carlo Transport Code, UCRL-ID-126455, Rev. 4, Lawrence Livermore National Laboratory, 2002.
[11] T.E. Booth, A Weight (Charge) Conserving Importance-weighted Comb for Monte Carlo, LA-UR–96-0051, Los Alamos National Laboratory, 1996.
[12] D.E. Cullen, C.J. Clouse, R. Procassini, R.C. Little, Static and Dynamic Criticality: Are They Different? UCRL-TR-201506, Lawrence Livermore National Laboratory, 2003.
[13] D. Brockway, P. Soran, P. Whalen, Monte Carlo α Calculation, LA-UR-85-1224, Los Alamos National Laboratory, 1985.
[14] C.H. Pyeon, Experimental Benchmarks on Thorium-loaded Accelerator-driven System at Kyoto University Critical Assembly, KURR-TR(CD)-48, Research Reactor Institute, Kyoto University, 2015.
[15] N. Shaukat, H.J. Shim, Alpha eigenvalue estimation from dynamic Monte Carlo calculation for subcritical systems, in: Transactions of the Korean Nuclear Society Spring Meeting, Jeju, Korea, May 11–13, 2016.
[16] H.J. Shim, S.H. Jang, S.M. Kang, Monte Carlo alpha iteration algorithm for a subcritical system analysis, Sci. Technol. Nucl. Ins. 2015 (2015) 859242. http://dx.doi.org/10.1155/2015/859242.
[17] H.J. Shim, B.S. Han, J.S. Jung, H.J. Park, C.H. Kim, McCARD: Monte Carlo code for advanced reactor design and analysis, Nucl. Eng. Technol. 44 (2012) 161–176.
[18] M. Aufiero, C. Fiorina, A. Laureau, P. Rubiolo, V. Valtavirta, Serpent–OpenFoam Coupling in transient mode: simulation of a Godiva prompt critical burst, in: Proceedings of ANS MC2015–Joint International Conference on Mathematics and Computation (M&C), Supercomputing in Nuclear Applications (SNA) and the Monte Carlo (MC) Method, Nashville, TN, 2015.
[19] J. Lieberoth, A Monte Carlo technique to solve the static eigenvalue problem of the Boltzmann transport equation, Nukleonik 11 (1968) 213–219.
[20] V.F. Boyarinov, P.A. Fomichenko, J. Hou, K. Ivanov, A. Aures, W. Zwermann, K. Velkov, Deterministic Time-dependent Neutron Transport Benchmark without Spatial Homogenization (C5G7-TD), Version 1.6, NEA/NSC/DOC(2016), OECD Nuclear Energy Agency, 2016.
[21] Y.S. Jung, C.B. Shim, C.H. Lim, H.G. Joo, Practical numerical reactor employing direct whole core neutron transport and subchannel thermal/hydraulic solvers, Ann. Nucl. Energy 62 (2013) 357–374.
[22] A.F. Henry, The application of reactor kinetics to the analysis of experiments, Nucl. Sci. Eng. 3 (1958) 52–70.
[23] A.F. Henry, Nuclear-Reactor Analysis, MIT Press, Cambridge, MA, 1975.
[24] E. Lewis, M. Smith, N. Tsoulfanidis, G. Palmiotti, T. Taiwo, R. Blomquist, Benchmark Specification for Deterministic 2-D/3-D MOX Fuel Assembly Transport Calculations without Spatial Homogenization (C5G7 MOX), NEA/NSC, 2001.